Study of TileCal Sampling Fraction for Improvement of Monte-Carlo Data Reconstruction

J.Budagov[1], G.Khoriauli[1], [2],
J.Khubua[1], [3], A.Khukhunaishvili[1],
Y.Kulchitsky[1], [4], A.Solodkov[5]

[1] *JINR, Dubna*
[2] *TSU, Tbilisi*
[3] *TSU HEPI, Tbilisi*
[4] *B.I. Stepanov Institute of Physics, National Academy of Science of Belarus, Minsk*
[5] *IHEP, Protvino*

Abstract

In this work we made a detailed calculation of Tile Calorimeter Sampling Fraction parameter (TSF) using single electron and pion Geant4 Monte-Carlo simulation of ATLAS hadronic calorimeter (TileCal) within ATHENA — common software framework of ATLAS. Our study was based on MC Truth data provided by special Geant4 MC simulation objects — Calibration Hits, design which was implemented in TileCal simulation by our group. We used this TSF value for reconstruction of TileCal single pions simulation data. It was done for ATLAS Combined test beam 2004 (CTB2004) configuration setup. Results of the reconstruction were compared with MC Truth and CTB2004 reconstructed experimental data. Good agreement between them shows quite evident improvement in TileCal MC data reconstruction of hadronic shower energy in electromagnetic scale.

†*Corresponding author. Tel : +7 49621 63523; fax : +7 49621 65324*
email : gia@mail.cern.ch (G. Khoriauli)

1   Introduction

One of the important tasks of ATLAS detector performance improvement is a hadronic calibration of the ATLAS calorimeter facility (Tile & LAr calorimeters). Hadronic calibration of the calorimeter is very crucial aspect in a study of physical processes with hadronic jet(s) production.

The goal of the hadronic calibration is to provide methods and their parameters for hadrons energy reconstruction in the calorimeter. The way to achieve this goal is a detailed Monte-Carlo study of the calorimeter response dependence on the impact hadron energy, pseudo-rapidity and comparison of MC results with experimental beam test data.

In a calorimeter only some part of hadron shower energy is responsible for the formation of calorimeter response. This is the energy deposited in the sensitive parts of calorimeter cells. We will also call it a visible energy or an energy in the electromagnetic scale (EM-scale).

The other part of the energy is lost because of several reasons. One of them is a non-compensation of the calorimeter caused by a hadronic shower energy loss in the nuclear breakup processes, which has a non-linear dependence on the impact hadron energy. This energy is also called as invisible energy because it will never contribute in a calorimeter response [1]. The relatively small energy loss is caused by the secondary particles escaped from ATLAS detector. They are mainly neutrinos and muons.

And finally, quite significant part of the energy is lost in Dead Materials (any materials outside calorimeter cells). Since the only way of DM (Dead Material) energy loss study is MC simulation the correct, explicit description of all DM plays very important role in a hadronic calibration of the calorimeter.

Hadronic calibration of the calorimeter should provide methods for applying DM, non-compensation and escaped energy corrections to the energy of hadronic clusters reconstructed in the electromagnetic scale.

So, certain general steps of the hadron energy reconstruction can be determined, which should be done before reconstruction and physical calibration of hadronic jets (see [1]):

- Provide hadronic shower energy reconstruction in the EM-scale (cell level energy reconstruction).

---

[1]This statement is true for "endothermic" nuclear breakups, when some external energy ($\geq$ bound energy) is needed to break a nucleus up. The "isothermal" nuclear breakup processes, when the bound energy becomes the kinetic energy of products are the additional sources of energy deposition in a calorimeter. So, these processes give contribution in the calorimeter response. However, "isothermal" nuclei breakup process happens very rarely in the calorimeter relatively to "endothermic" one and can be neglected.

- Apply calorimeter non-compensation and escaped energy corrections.

- Apply Dead Material energy corrections.

The last two steps are objects of a calorimeter hadronic calibration study. But they need to be based on the right results from the first step. It's clear that before applying the hadronic level corrections response energy in EM-scale should be correctly reconstructed.

There was a lot of reports and publications (see, for example, [2]) dedicated to the study of ATLAS TileCal calorimeter electromagnetic scale based on the data from several Test Beam activities.

One of the main problem within this issue until now was quite significant difference between the results of energy reconstruction in EM-scale for TileCal MC data and beam test experimental data.

The goal of this work was to study and explain the reason of this discrepancy using newly designed hadronic calibration software for ATLAS MC simulation known as Calibration Hits, design which was implemented in TileCal simulation by our group [3].

Our study of this problem led us to the recalculation of Tile Sampling Fraction parameter. This parameter is used in the digitization step of MC simulation. The new TSF value significantly improved reconstruction results in comparison with MC truth and experimental CTB2004 data.

2   Calorimeter Geant4 based simulation with Calibration Hits

Monte-Carlo simulation of the ATLAS calorimeter plays very important role in studying of a hadronic shower behavior in the calorimeter. For a calorimeter hadronic calibration purposes special hadronic calibration algorithms were designed within the common ATLAS software framework, ATHENA. This included a developing of the readout geometry for Dead Material pseudo-cells and the special Geant4 simulation Hit-objects, called Calibration Hits.

Calibration Hits have three important differences from the ordinary Hit objects recorded in a ordinary Geant4 simulation of ATLAS calorimeter. They are:

- Contrary to ordinary hits, which are provided only for calorimeter cells Calibration Hits are also provided for DM pseudo-cells.

- Calibration Hit records the energy from any materials of a cell or DM pseudo-cell, while an ordinary Hit object contains only the

energy deposited in the sensitive materials of the calorimeter cell. These sensitive materials are scintillators in the TileCal or liquid argon in the LAr calorimeter.

- Unlike an ordinary Hit, which records only deposited (visible) energy, Calibration Hit records any kind of shower energy loss and classifies it into four different components: electromagnetic, non-electromagnetic, invisible and escaped energies. Electromagnetic and non-electromagnetic energies together are a visible part of shower energy and they are responsible for a calorimeter response.

As it has been already mentioned Calibration Hits can be associated with Dead Material pseudo-cells also. For this purpose a special readout geometry was developed for DM with sub-calorimeters corresponding granularity (for TileCal it is — $\Delta\eta \times \Delta\phi = 0.1 \times 0.1$).

All these characteristics make Calibration Hits technique very powerful tool in calorimeter performance study. First of all, Calibration Hits give a direct access to the MC total energy loss in any calorimeter cells. Moreover, there is a direct access to these different components of total energy loss in the cells: $\mathbf{E_{EM}}$ — electromagnetic, $\mathbf{E_{NonEM}}$ — non-electromagnetic (both together are a visible energy), $\mathbf{E_{Invis}}$ — invisible and $\mathbf{E_{Esc}}$ — escaped energies. "Direct access" means that energy components stored in Calibration Hits can be simply copied in Ntuple.

We used Geant4 based MC simulation with Calibration Hits to calculate TSF and to get MC truth for shower energy in EM-scale (the same as visible energy or deposited energy in TileCal cells). This last was compared with the results of energy reconstruction in EM-scale for MC data. The significant agreement between MC truth and MC reconstruction for the energy in EM-scale has been achieved after using the new TSF value.

The simulation and reconstruction of MC data were carried out with Atlas Release 10.0.2 (Geant4 v7.0). More details of the simulation are given below.

- Details of single electron simulation in ATLAS:

    - Physics List — QGSP_GN with 1 mm Range Cut[2].
    - All sub-detectors and additional materials in front of TileCal were removed from the simulation. This allowed electron beam to reach TileCal modules with a very negligible energy loss on their trajectory in the air toward TileCal (fig.1).

---

[2]Defines a particle kinetic energy low threshold to allow this particle for a tracking by Geant4.

- For electron beam energies in the simulation we took the values corresponding to the CTB2004 electron beam energies: 20, 50, 100, 180, 250, 350 GeV.

- A detailed scan by η (pseudo-rapidity) of TileCal modules was done. First, we simulated 4 k events for each beam energy with flat η-distribution η in the η-range $0.00 - 0.8$. The electron vertex Z-coordinate (Z is the axis along the ATLAS beam pipe) had Gaussian distribution with $Z_{mean} = 0$ and $\sigma(Z) = 5\ cm$. Further, we made simulation at several fixed η points with the same Gaussian distributed vertex along Z. Fixed η values were taken with a step $\Delta\eta = 0.02$ in η range $0.00 - 0.80$ (TileCal central barrel). 1 k events were simulated in each run.

- Details of single pion simulation in CTB2004:

  - Physics List — QGSP_GN with 1 mm Range Cut

  - Partially combined setup was taken for the CTB2004 detectors configuration, LAr + TileCal only.

  - For pion beam energies in the simulation we took values corresponding to the CTB2004 single pion beam energies, 20, 50, 100, 150, 180, 250, 350 GeV.

  - The following η values were taken to scan TileCal central barrel modules: 0.05, 0.15, 0.20, 0.25, 0.35, 0.45, 0.55, 0.65.

  - 1 k events were simulated in the each run.

3 Tile Sampling Fraction

TSF characterizes deposited (visible) energy sharing between sensitive and non-sensitive parts of TileCal cells. It is the average ratio of total deposited energy in the cells over the energy deposited in scintillators [3].

$$TSF = \frac{E_{cells}^{vis}}{E_{scint}^{vis}} \ , \tag{1}$$

where, E_{cells}^{vis} — energy deposited in TileCal cells E_{scint}^{vis} — energy deposited only in sensitive parts of cells (scintillators).

---

[3]There is also another definition of Tile Sampling Fraction, which is just the inverted quantity of our definition. For convenience, we defined TSF as it is directly used in TileCal MC data reconstruction
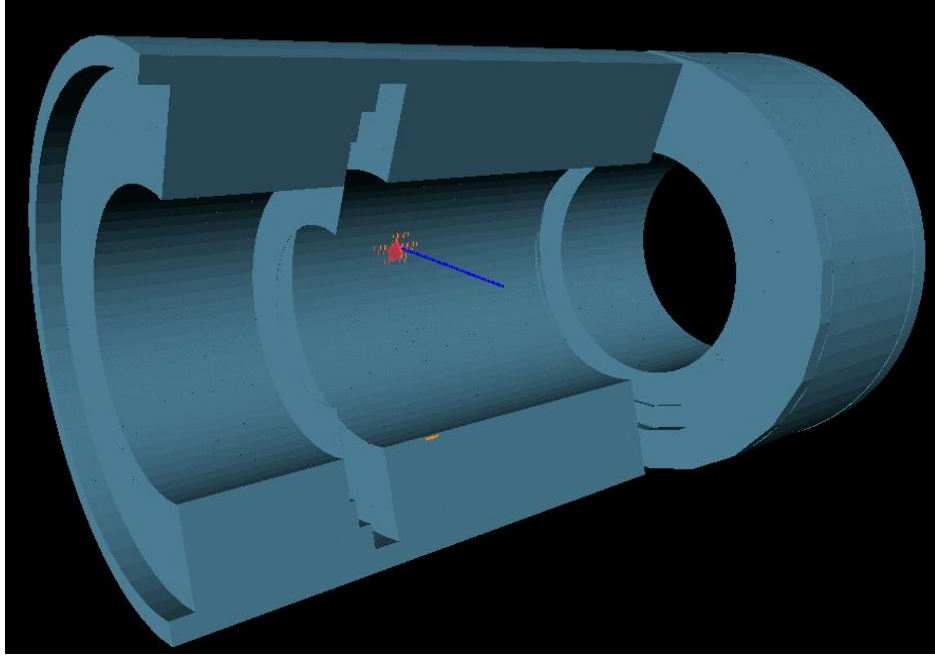
Figure 1: TileCal view with electron track and hits (GeoModel HitDisplay)

TSF strongly depends on the TileCal geometry structure. In particular, there is a dependence on the averaged ratio of absorber and scintillators volumes on the direction of a shower development. As it will be shown below there is a clear dependence between TSF and the ratio of electron shower paths in absorber iron and scintillators. It is already well known that TileCal has a structure (fig. 2 a), where the fluctuation of $Path_{abs}/Path_{scint}$ caused by small shift of Z-coordinate of impact point depends on the η region [4, 5]. The more this ratio the more energy lost in absorber (fig. 2 b). So, the local TSF value fluctuates significantly (fig. 3).

This behavior of TSF can be explained by the relatively tiny electron shower size. Molier's radius for electrons in Iron is $\approx 16.6mm$ [6, pg.170], [7], which is less than the width of one TileCal structural period in Z – 18.26 mm. So, electron "fills" TileCal structure within the sizes of one TileCal period.

TSF is expected do not depend on the particle initial energy since it characterizes the distribution of deposited energy between absorbers and sensitive materials but not the amount of this deposited energy. Though one can note a clear dependence on the impact particle energy for the average TSF value (fig. 3). The point is that the more particle energy
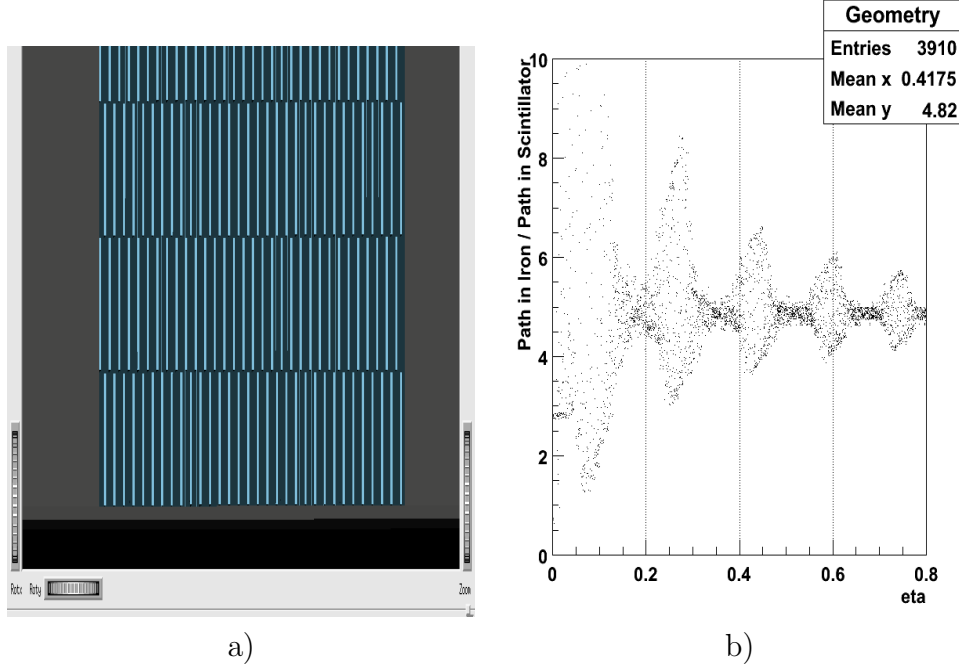
Figure 2: a) Sketch of TileCal Z-periodical structure for central barrel module. Blue volumes are scintillator tiles. b) Dependence of $Path_{abs}/Path_{sci}$-ratio on η for first A-sampling of a central barrel module.

is, the further shower passes and the more particle "feels" the periodical structure of TileCal. In other words, TSF value becomes more sensitive to the TileCal geometry at higher energies.

To calculate TSF for whole TileCal central barrel region, first of all, we calculated a set of local TSF_{mean} at fixed η — values. Z-coordinate of electron beam vertex was varied in the range of several TileCal periods (see simulation details in the previous section). In this case variation of local TSF is defined by the Z-periodical structure of TileCal and can be described by the formula [4]:

$$TSF \;=\; \frac{E_0}{E_{scint} - A_{scint}\cdot\sin(kz)} = \frac{E_0}{E_{scint}}\left(1 + \frac{A_{scint}}{E_{scint}}\cdot\sin(kz) + \dots\right) =$$

$$= TSF_{mean} + A_{TSF}\cdot\sin(kz)\;, \tag{2}$$

where, E_0 — total deposited energy in cells. for electrons in TileCal it's $\cong E_{beam}$; E_{scint}, A_{scint} — energy deposited in scintillators and its variation amplitude; $k = \frac{2\cdot pi}{period}$ $[mm^{-1}]$.

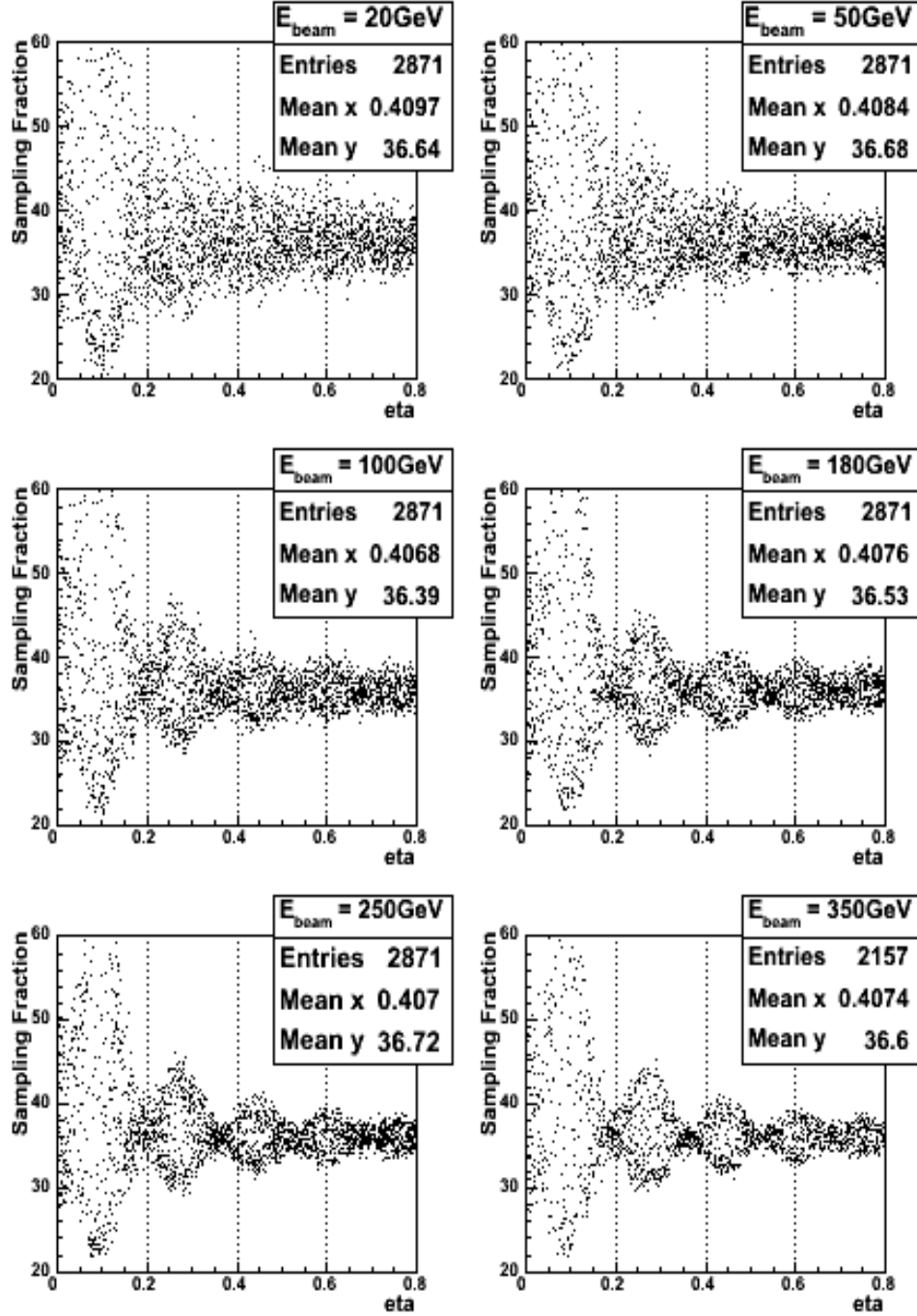[4]Using the expansion: $1/(1-x) = 1 + x + x^2 + x^3 + x^4 + ...$; for $|x| < 1$

6

Figure 3: Dependence of TSF on η for different electron beam energies. Correlation between TSF and $Path_{abs}/Path_{sci}$ oscillations increases with energy.
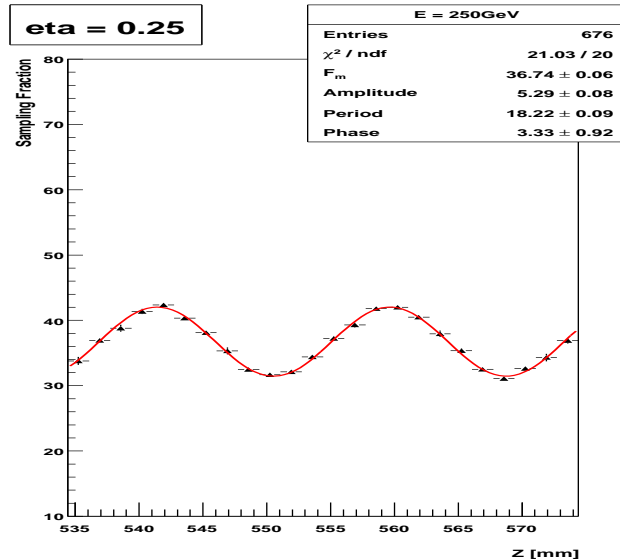
7

Figure 4: Local TSF variation (example plot at $\eta = 0.25$ for $E_{beam} = 250$ GeV) is defined by the Z-periodical structure of TileCal modules.

Fig. 4 Shows an example of local TSF variation as a function of Z-impact point fitted with the formula (2).

Fig. 5 Shows distribution of the periods of local TSF variation as a function of η for different beam energies. As it is clear from these plots the local periodicity of TSF variation is completely defined by TileCal Z-periodical structure and reminds a constant, $period \approx 18.2(6)\ mm$.

Dependencies of local TSF_{mean} and its variation amplitude on η have quite complicated structures (fig. 6 – fig. 8). It's clear that this behavior is defined by the geometrical feature of TileCal structure shown on the fig. 2 b. We call it — "η depended structure".

To describe the amplitude dependence on η we derived the following formula,

$$A_{TSF}(\eta) = \alpha R(\eta) \cdot \left(1 + \beta \sin^2(\eta \cdot \omega(\eta)) \right) \qquad (3)$$

where,

$$R(\eta) = \frac{\eta}{1 + A_1\eta + A_2\eta^2} \ ,$$
$$\omega(\eta) = \omega_0(1 + \alpha_\omega\eta) \ .$$

Rational function $R(\eta)$ is needed to describe a fast increase of the amplitude in the η-range $0.0 - 0.1$ and its further dumped oscillation (fig. 6).
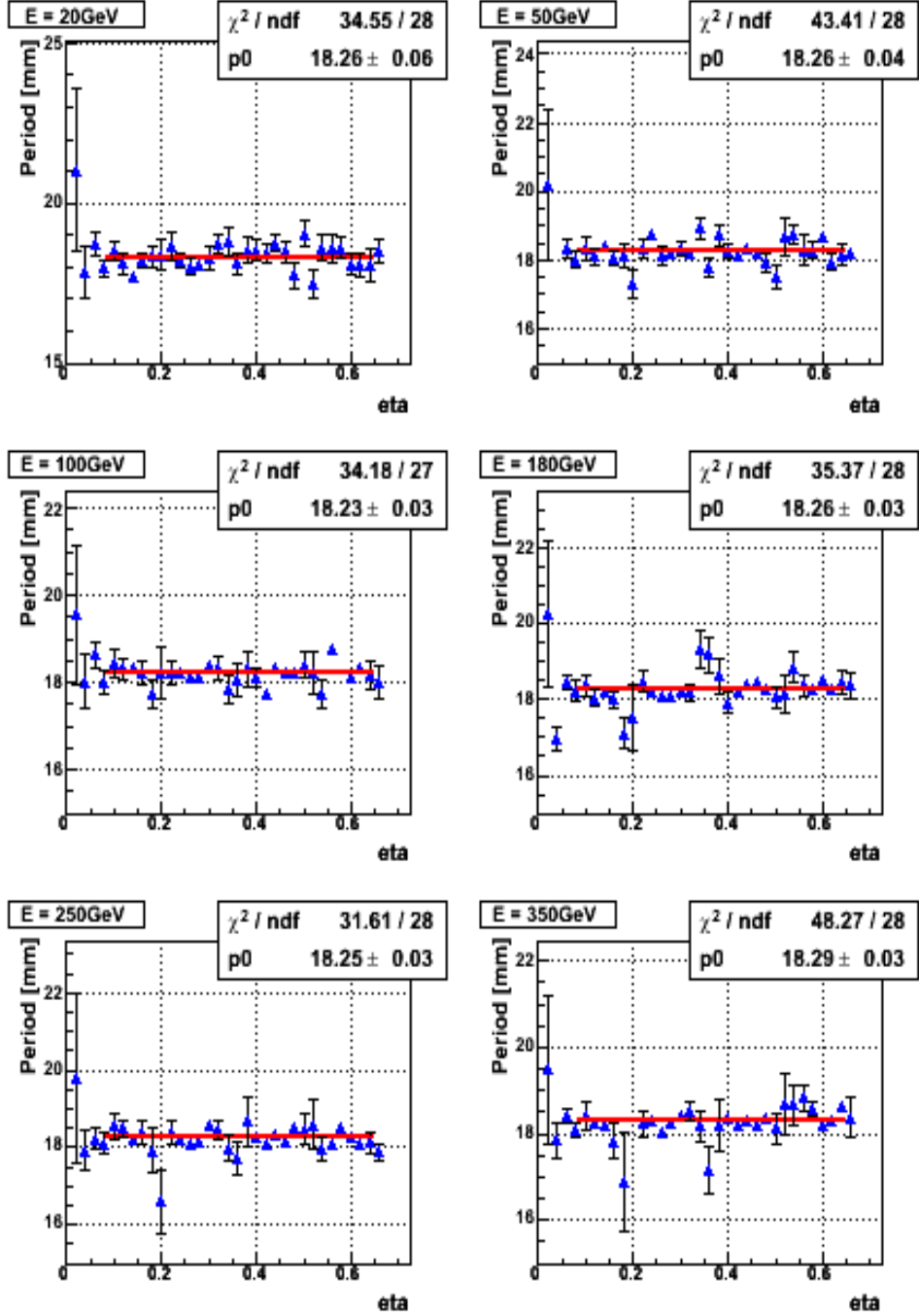
8

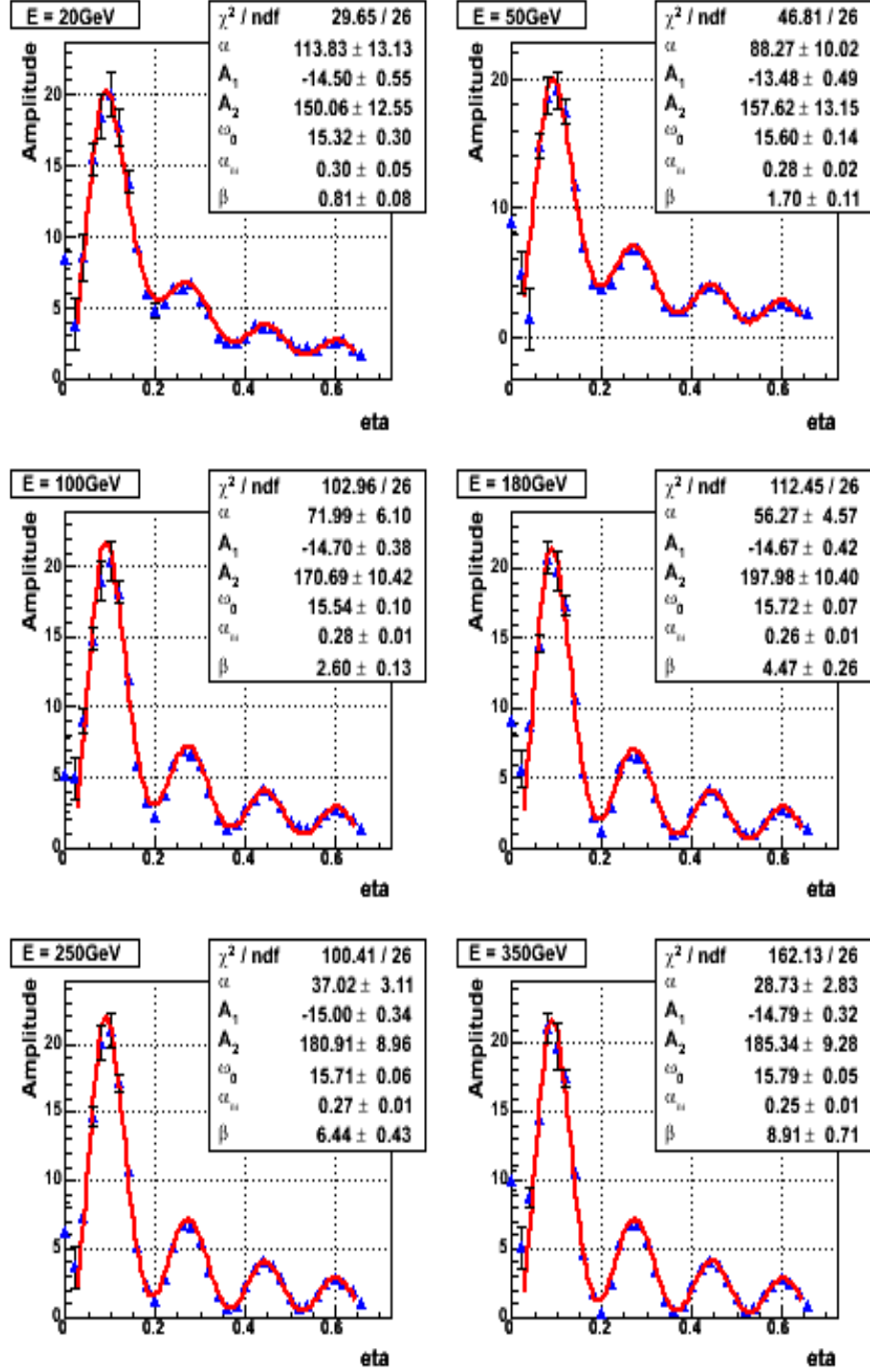Figure 5: Period of local TSF variation as a function of η for different E_{beam}.

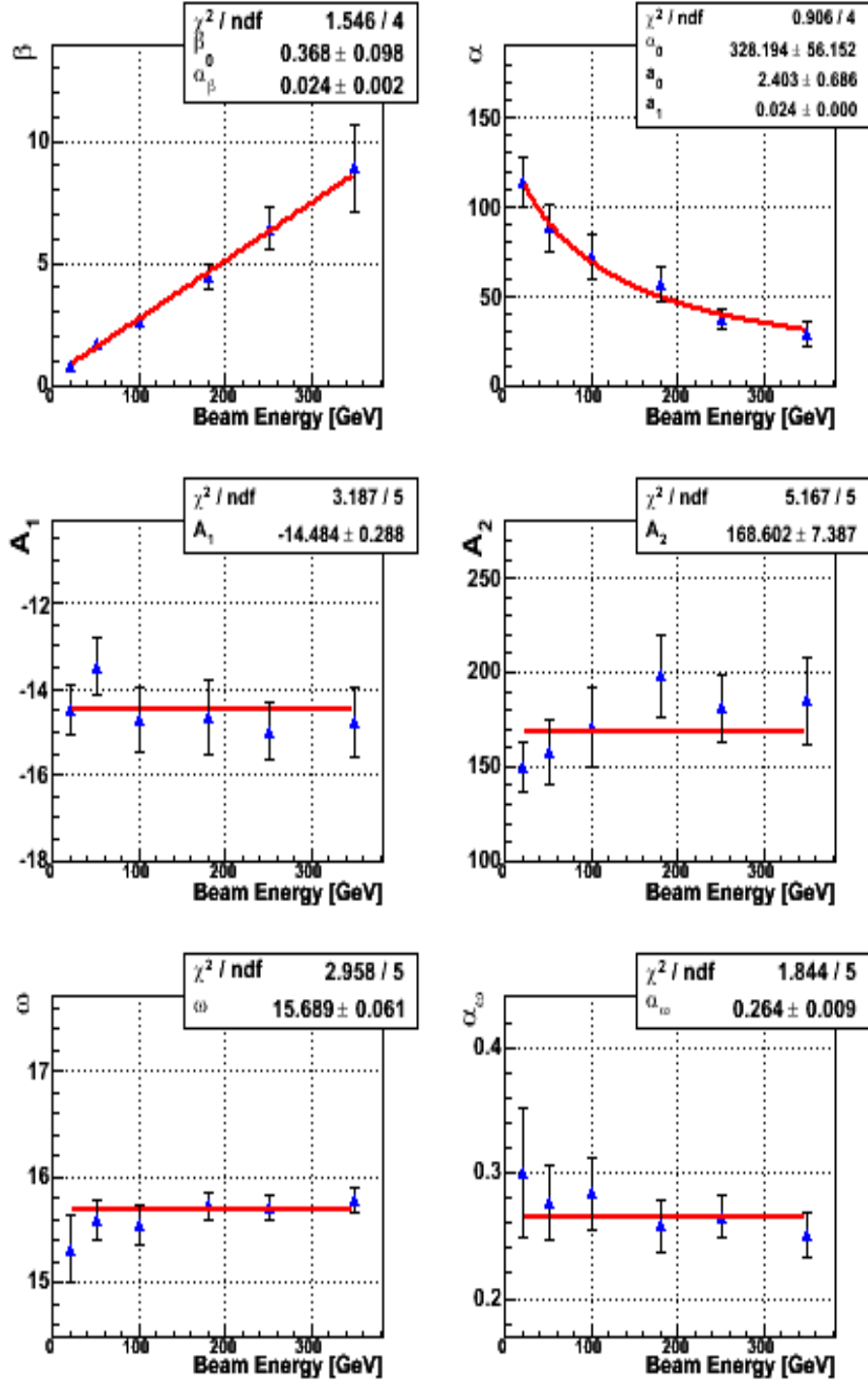Figure 6: Local TSF variation amplitude, A_{TSF}, dependence on η.

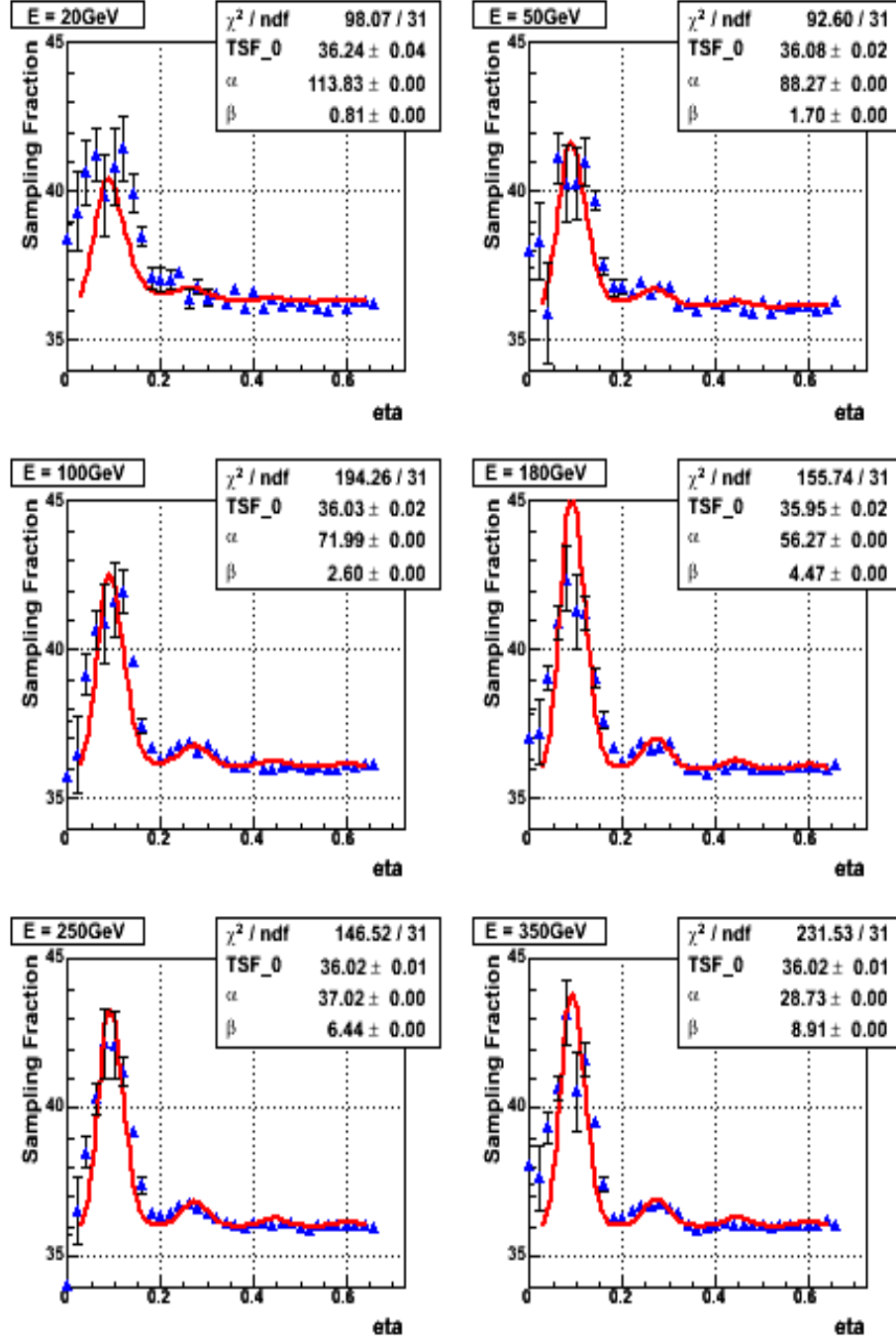Figure 7: Parameters of local TSF variation amplitude fit.

Figure 8: TSF_{mean} dependencies on η for different beam energies and corresponding fits by formula 4.

Fig. 7 shows the amplitude fit parameters at different beam energies. All parameters except β and α are beam energy independent. They are characterizing TSF dependence on η and are completely determined by TileCal geometry structure.

Parameter β increases linearly as the beam energy increases. This defines the sharpness of TSF oscillating behavior at higher beam energies since α decreases so that the spread of TSF value reminds almost the same for every beam energy (fig. 6)

Such fluctuating behavior of the amplitude can be explained in terms of the phase shift between adjacent layers (tiles) of the TileCal module. Maximum value of the amplitude corresponds the case when these layers are in the same phase for a given η, i.e. for example, for the first peak at $\eta = 0.1$ electron passes through the scintillators or irons of all layers at the same time. Minimum (about zero) value is achieved when adjacent layers are in the opposite phases, i.e. if electron enters the scintillator in the first layer, it will pass through the iron in the second layer and vice versa, so that the total path of the shower in scintillators and Iron is about the same for all electrons with this eta value regardless of point of entry in the TileCal.

As we have already seen (fig. 5) the period of TSF local variation doesn't depend on η. We used this fact to calculate TSF for whole η-region using the same expansion (formula (2)) with already defined amplitude. However, we kept more higher order members in the expansion since the TSF variation amplitude has the same order of magnitude as TSF itself. Then mean TSF (fit of the distribution of local TSF_{mean} values) is equal to the following[5]:

$$\langle TSF \rangle = TSF_0 \cdot \left(1 + \frac{1}{2} \left(\frac{A_{TSF}}{TSF_0} \right)^2 + \frac{3}{8} \left(\frac{A_{TSF}}{TSF_0} \right)^4 \right) , \qquad (4)$$

where, TSF_0 is a single free parameter of the fit. All other parameters were fixed because they were already defined from A_{TSF}-amplitude fit. The results of TSF fit are shown on the fig. 9.

For parameter TSF_0 we got the value (averaged by the beam energies),

$$TSF_0 = 36.03 \pm 0.03 .$$

The reason why we keep higher order dependent corrections in formula (4) is that the size of electromagnetic shower is comparable with Z-period of TileCal geometry structure. TSF_0 is the estimation of TSF if we do not consider its variation caused by the "η depended structure".

---

[5]Considering that mean values of odd-order $sin(kz)$ terms of the expansion vanish.
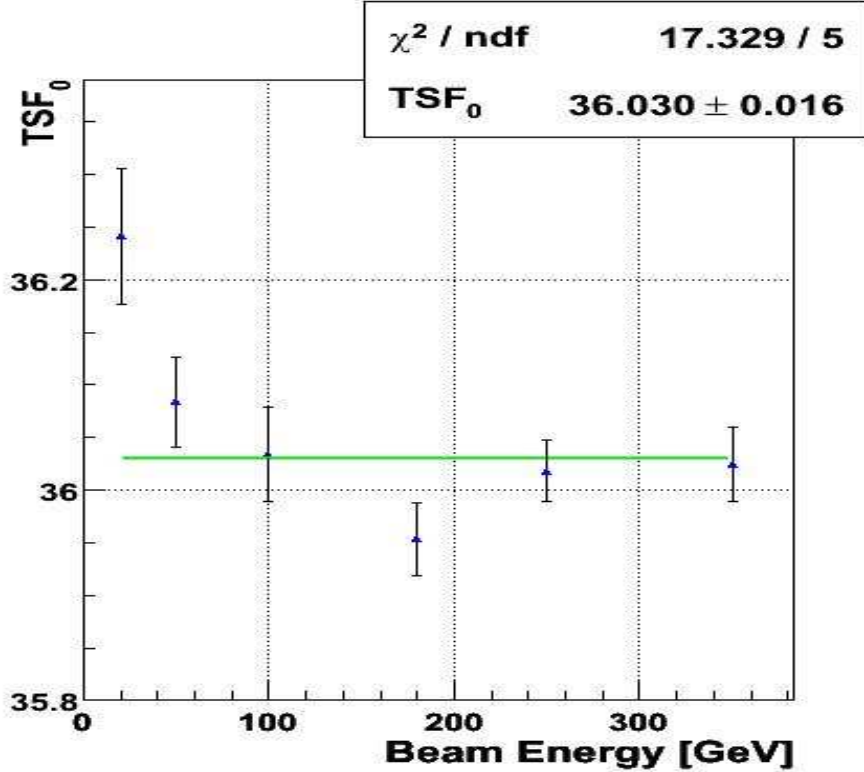
Figure 9: Estimation of TSF_0 as a function of electron beam energy

This is the case of hadronic shower in TileCal, which has quite large size rather than electron shower. As we will see below TSF calculated on pions response is almost the same as TSF_0.

One more important note we would like to make is concerned to calculation of electromagnetic constants for TileCal cells. From the previous plots for TSF and its amplitude one can define "good" and "bad" η values related to electron response behavior. We suggest that in the experimental case of electromagnetic constants calculation for TileCal cells only "good" η-s should be used for the calculation. In this case experimental response will have good Gaussian distribution shape contrary to "bad" η cases, when there is quite big and complicated fluctuations of electron response (reflected in the behavior of TSF and its variation amplitude), which potentially leads to the error in calculation of cells electromagnetic constants and therefore to an error in a definition of the whole TileCal EM-scale.

As an alternative way we calculated TSF from the single pion simulation. As long as Calibration Hits give a possibility to separate visible
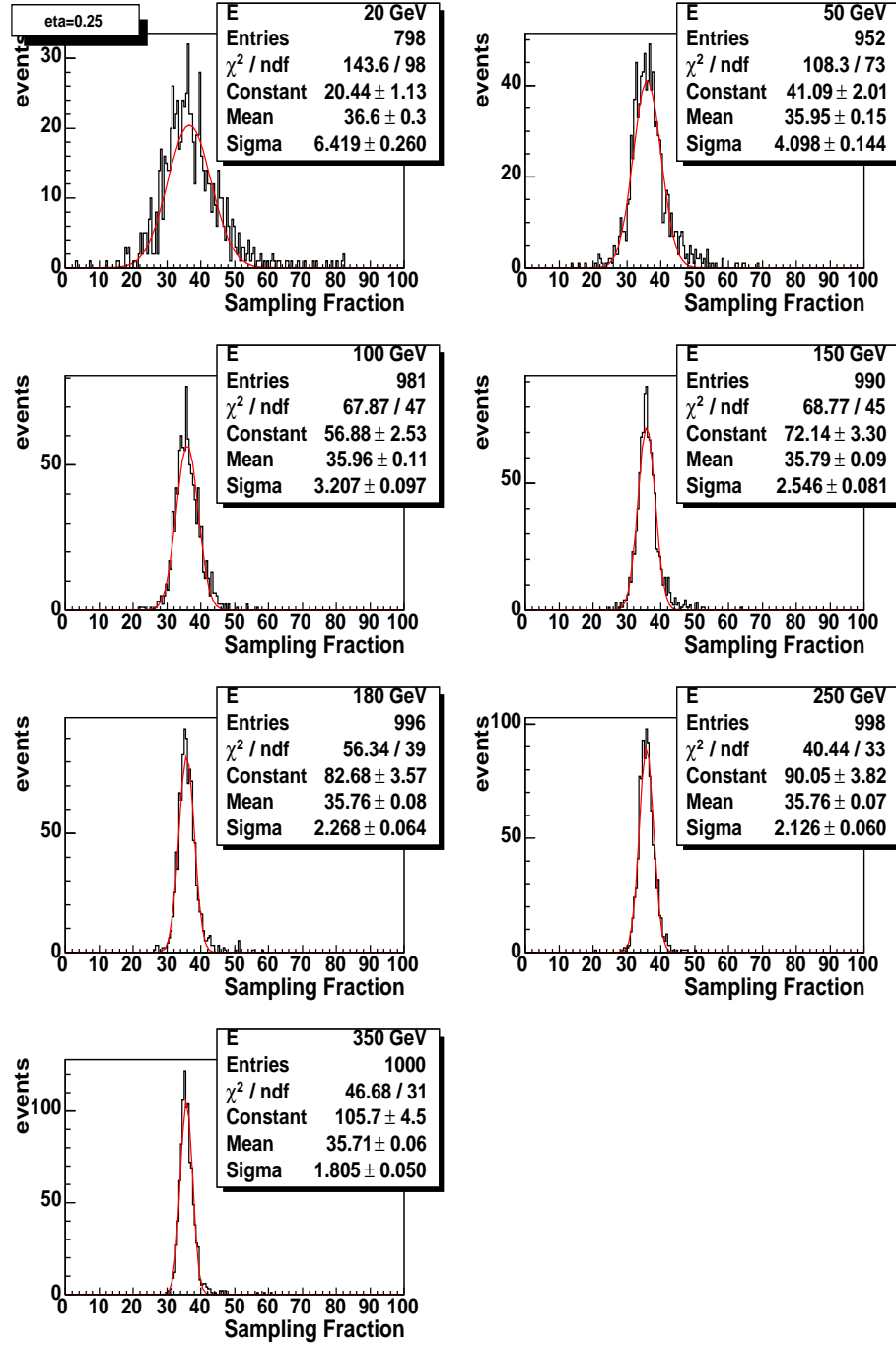
14

Figure 10: Gauss-distributed TSF calculated on a pion response for different beam energies at $\eta = 0.25$.

energy part from a pion shower total energy it's possible to calculate TSF as the ratio with using formula (2).

Unlike electron shower, where the electromagnetic energy fully dominates in shower, pion shower visible energy part is the sum of electromagnetic and non-electromagnetic (hadrons, muons and etc.) energies. Therefore, one can't make an assumption that TSF calculated on pion response will be the same as TSF for electron because sharing of non-electromagnetic energy between Tile cell absorber and sensitive materials might be different from the electromagnetic one. However, as we will see below sampling fractions are the same for both kinds of shower energies.

Fig. 10 shows TSF calculated at $\eta = 0.25$ for different beam energies. Unlike the electron case pion TSF distribution is well described by Gauss. The reason of this behavior is that pion shower has significantly larger size than electron one and TileCal intrinsic η non-homogeneous structure doesn't influence anymore.
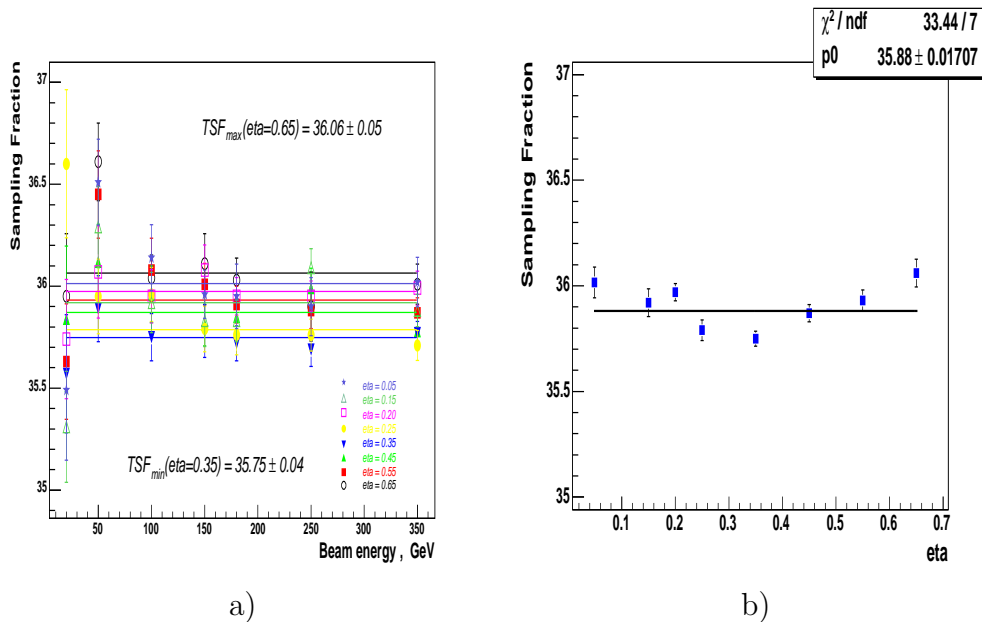

Figure 11: a) TSF dependence on beam energies for η-region $0.05 \div 0.65$. b) TSF averaged over beam energies for the same η-region.

TSF dependence on beam energy calculated at several η points for Tile central barrel region is shown on the fig. 11 a. Table 1 provides the results of the fits. These average values and a result of the fit by constant are presented on the fig. 11 b.

Finally, for TSF we got the value,

$$TSF_{had} = 35.9 \pm 0.4$$

Table 1: Averaged TSF values for different η.

η	0.05	0.15	0.20	0.25	0.35	0.45	0.55	0.65
TSF	36.01 $\pm$ 0.07	35.92 $\pm$ 0.07	35.97 $\pm$ 0.04	35.79 $\pm$ 0.05	35.75 $\pm$ 0.04	35.87 $\pm$ 0.04	35.93 $\pm$ 0.05	36.06 $\pm$ 0.07

This result is quite close to TSF_0 calculated on the electron response. This indicates that a non-electromagnetic part of hadronic shower contributes in the formation of a Tile calorimeter response with same energy sharing between sensitive and absorber materials as an electromagnetic part of shower does.

4   MC reconstruction results

We made a reconstruction of MC simulation data two times. Once this was done with using of TSF old value and second time with the new one. All other parameters were absolutely the same in both cases as long as the goal was to study how the only new TSF could improve agreement between MC reconstruction results and MC truth for TileCal central barrel. Comparison of these new results with reconstructed CTB2004 experimental data will be also shown in the next section.

Reconstruction of the energy in EM-scale was done using the TopoClustering algorithm with 4-2-0 schema of noise suppression (Atlas Release 10.0.2). The visible part of Calibration Hits energy was taken for the comparison because it can be considered as MC truth for energy deposition in calorimeter. Meanwhile, visible energy in each event was summed only from those Calibration Hits, which corresponding cells were also included into TopoClusters in the same event.

Fig. 12 shows illustrative plots how the agreement between MC reconstruction and MC truth was improved with new TSF (plots on the right column) in comparison of the results with old TSF (plots on the left column).

Fig. 13 shows fitted results for "old" and "new" relative differences between MC truth and reconstruction as a function of beam energy. Plots for eight η-s are shown. The corresponding fit results are provided in the table 2. These results show that new TSF in TileCal MC reconstruction significantly reduced the existing disagreement between MC truth and MC reconstruction.

The averaged (over all beam energies) result for the difference as a function of η is shown on the fig. 14. Finally, we got the following
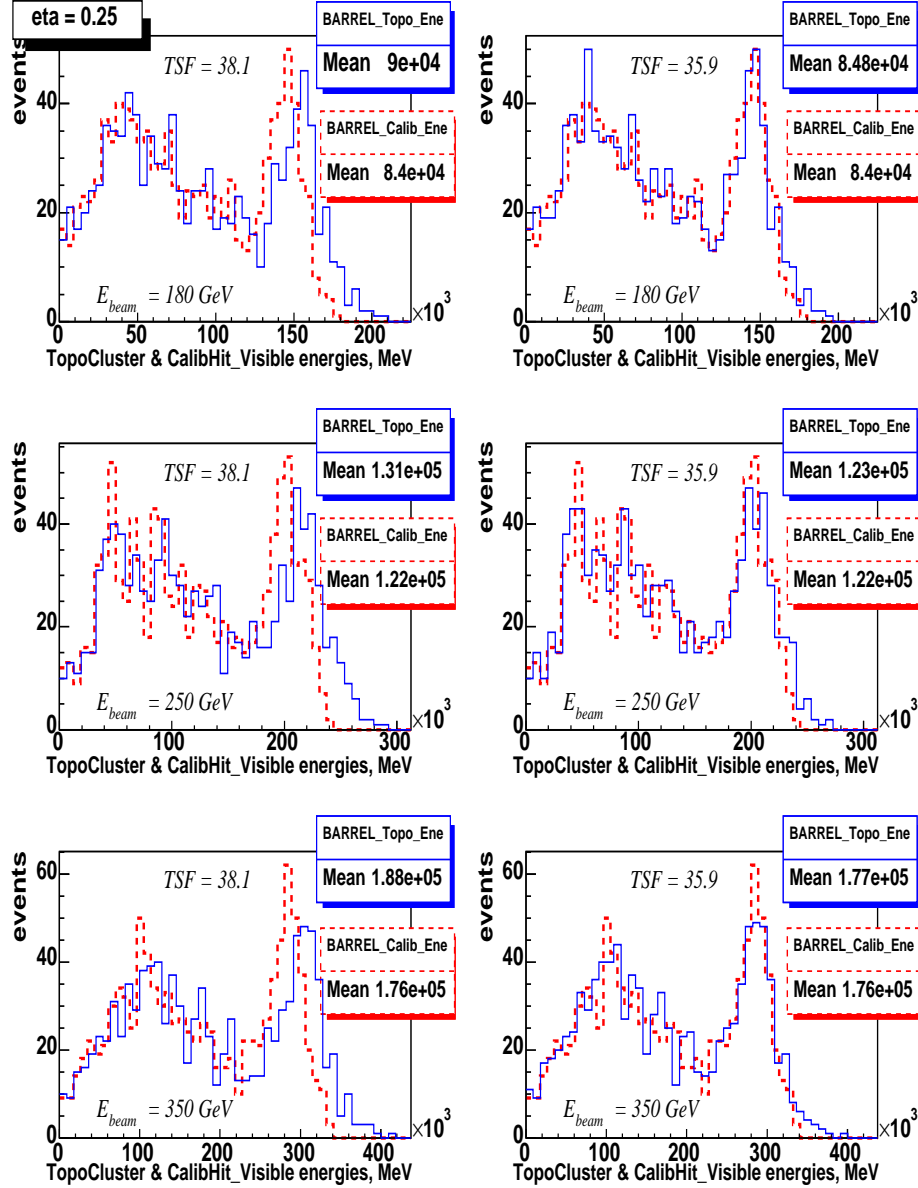
Figure 12: Comparison of MC truth (dashed line) and MC reconstruction (solid line) with old (plots on the left) and new (plots on the right) TSF. X-axis represents the energy in TileCal barrel reconstructed in EM-scale and the visible part of corresponding Calibration Hits energy in barrel. Similar comparisons were done for different beam energies and η. The results for $\eta = 0.25$ are shown.
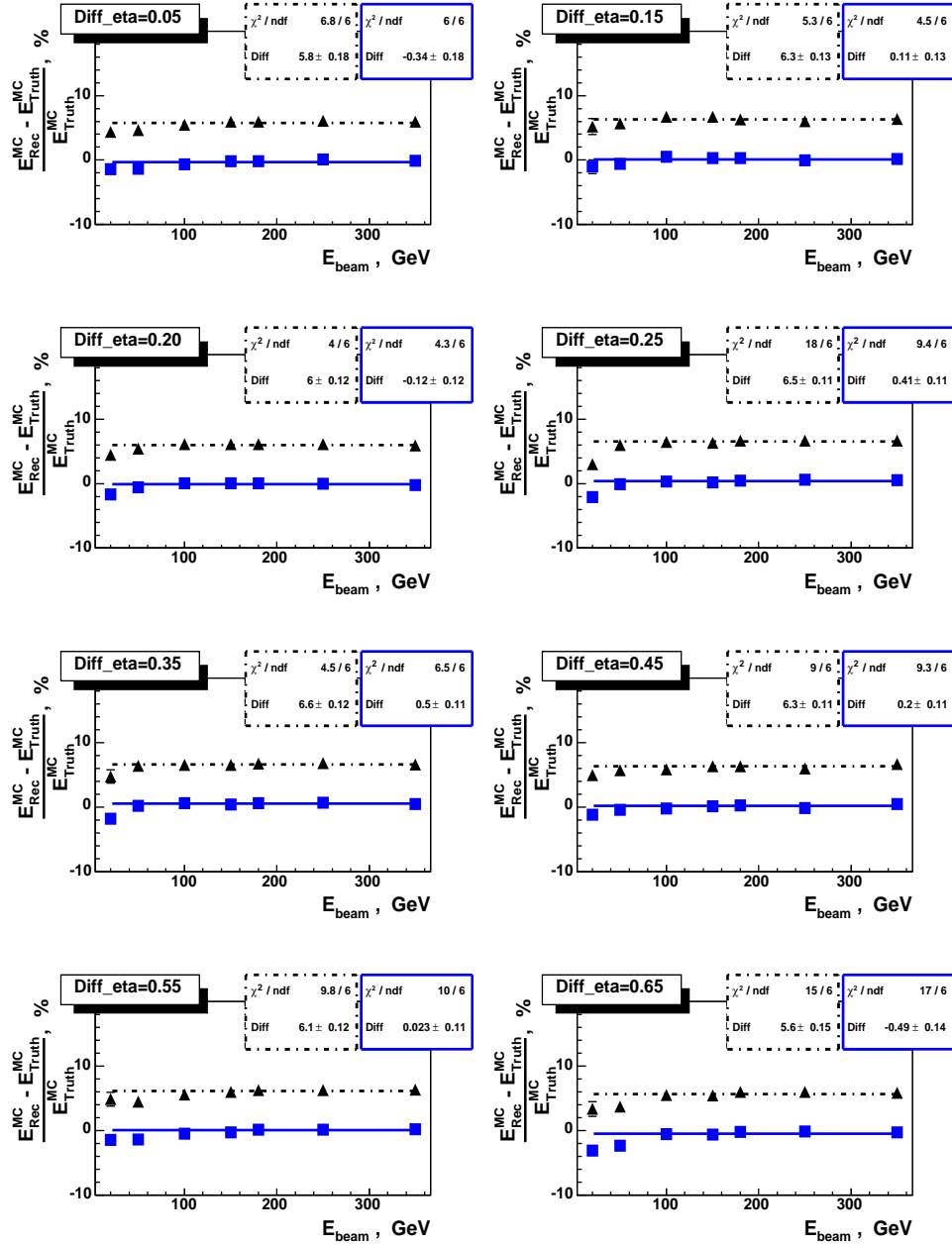
Figure 13: Relative difference between MC Truth and MC reconstruction with old (triangles) and new (squares) TSF in TileCal MC reconstruction. Difference is calculated event-by-event for each energy-η point.
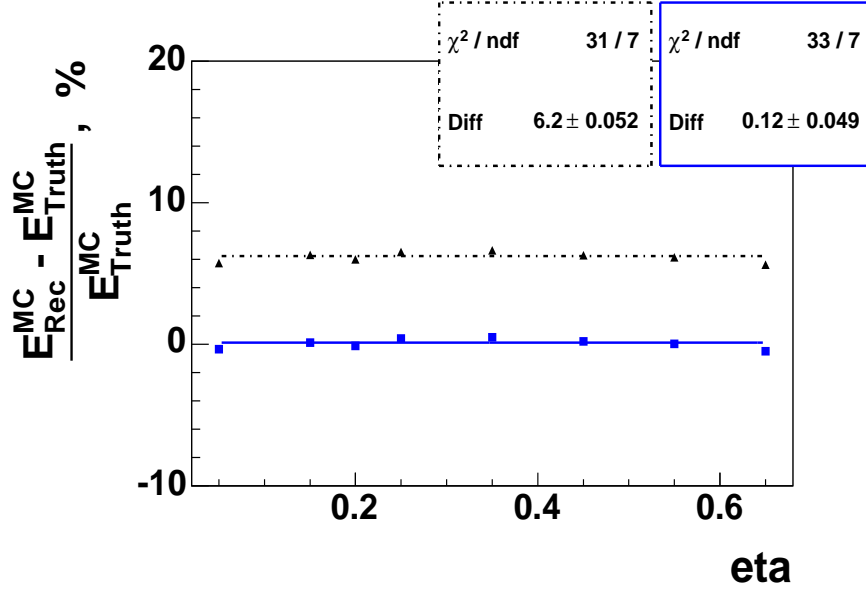
Figure 14: Relative difference between MC Truth and MC reconstruction as a function of η. Triangles are for the MC reconstruction with old TSF and squares are for the new TSF case.

averaged estimation of the difference in case of old and new TSF,

$$diff(old) = 6.2 \pm 0.1\%$$

$$diff(new) = 0.12 \pm 0.11\%$$

Table 2: Difference between MC truth and reconstructed MC energy in case of old and new TSF.

η	0.05	0.15	0.20	0.25	0.35	0.45	0.55	0.65
Diff, % TSF=38.1	5.8 $\pm$ 0.2	6.3 $\pm$ 0.13	6.0 $\pm$ 0.12	6.5 $\pm$ 0.19	6.6 $\pm$ 0.12	6.3 $\pm$ 0.14	6.2 $\pm$ 0.15	5.7 $\pm$ 0.23
Diff, % TSF=35.9	-0.3 $\pm$ 0.18	0.1 $\pm$ 0.13	-0.1 $\pm$ 0.12	0.4 $\pm$ 0.13	0.5 $\pm$ 0.12	0.2 $\pm$ 0.13	0.02 $\pm$ 0.14	-0.5 $\pm$ 0.23

5 Comparison of MC with CTB2004 Experimental data

As we already saw in the previous section, quite good agreement between truth and reconstructed MC data has been reached after we used new TSF. But a reliability of MC results is defined by their agreement with the experimental results. Therefore, it was quite important to compare new MC results with the experimental results of CTB2004. For this purpose we used single pion experimental data reconstructed with the same Atlas Release 10.0.2 for the CTB2004 runs given in table 3. In the time of writing this note those experimental data were stored at this address: **/castor/cern.ch/grid/atlas/datafiles/ctb/realdata/10.0.2.v3/**

Table 3: Used CTB2004 single pion runs.

η	E_{beam} (GeV)						
	20	50	100	150	180	250	350
0.25	2100481	2100177	2100173	2100171	2100164	1002175	1004222
0.35	2100482		2100348	2100449	2100445	1004014	
0.45	2100494	2100300	2100292	2100274	2100318		
0.55	2100501	2100362	2100352	2100426	2100422		

Unlike MC data the experimental data for single pions were contaminated by muons and electrons. On the fig. 15 there is an example of this contamination. The dotted histogram on the first plot represents calorimeter TopoClusters energy distribution without cuts against muons and electrons (only not-physical events with extremely high response were removed). The dot-dashed Gauss distributed histogram shows the pions energy after applying the cuts. The middle and bottom plots are representing TopoClusters energy distributions (also after applying the cuts) in TileCal central barrel and LAr EM barrel respectively.

Fig. 16 shows a distribution of TileCal central barrel TopoClusters energy for experimental and MC reconstructed data and also MC truth from Calibration Hits. Plots for different energies at $\eta = 0.25$ are shown. This is the region where we have got the best agreement between these three types of data. We can say that the TileCal MC model describes the experiment quite well.

The next step of this work was a study of TileCal performance for pions, which passed LAr EM barrel as Minimal Ionizing Particles (MIP). So, we selected pions, which started developing the hadronic shower either in TileCal barrel or in the Dead Material after LAr sensitive region. Fig. 17 shows an example of the distribution of pions deposited energy
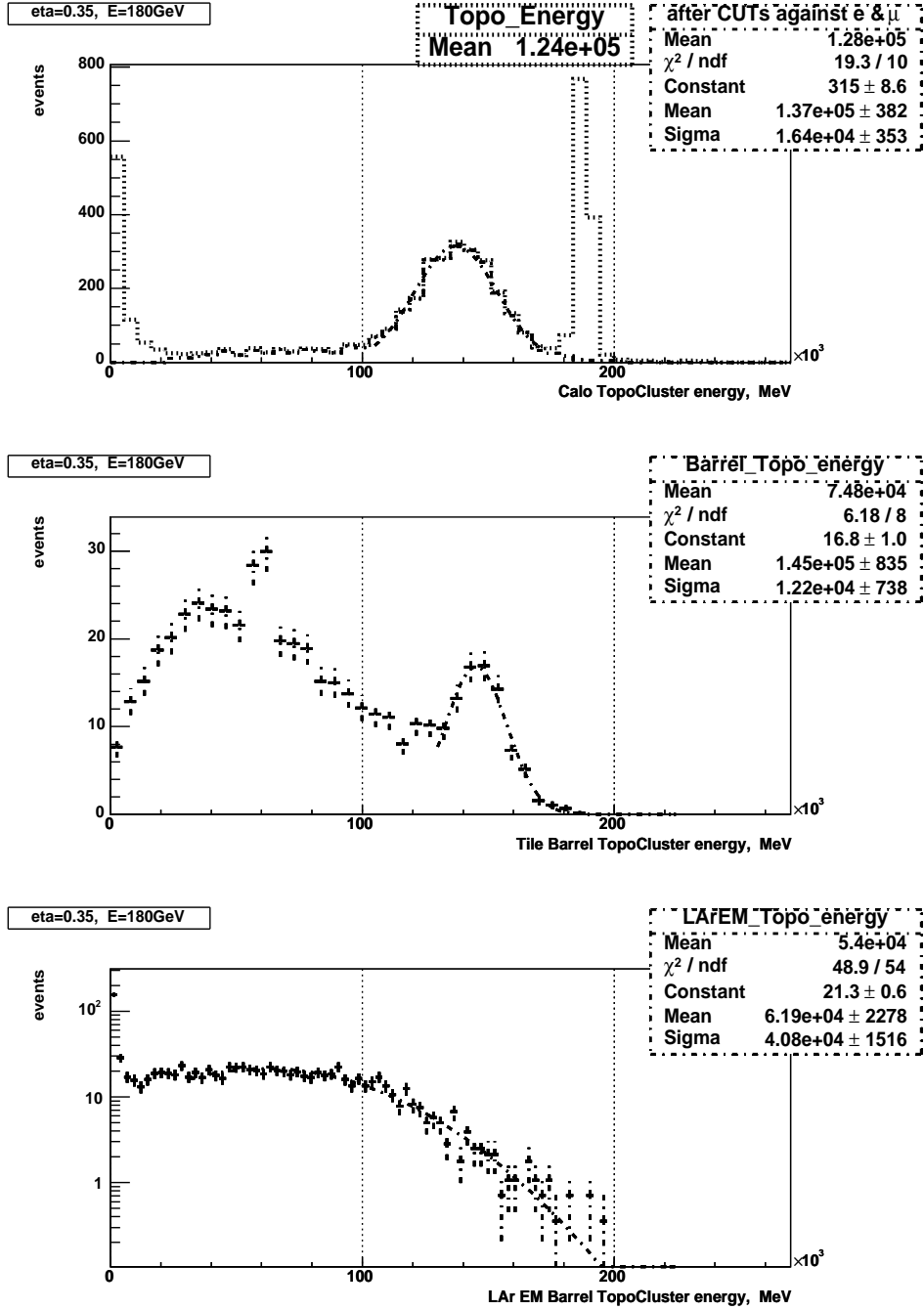
Figure 15: Upper plot is TopoCluster energy distribution before(dotted) and after(dash-dotted) applying cuts against muons and electrons. Next plots are TopoCluster energy distributions in TileCal central barrel and LAr EM barrel respectively after applying those cuts. $E_{beam} = 180$ GeV, $\eta = 0.35$
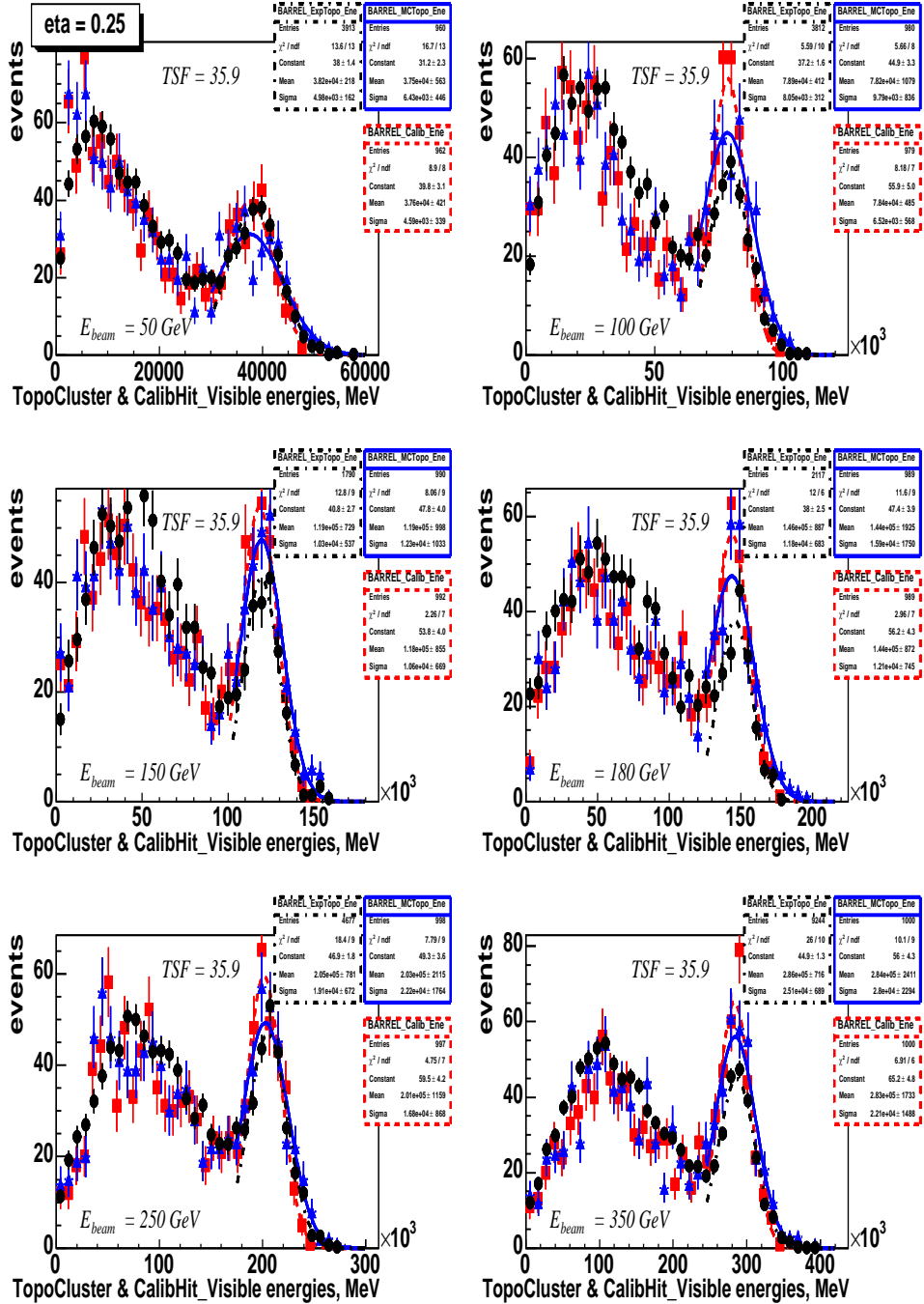
22

Figure 16: Distribution of TileCal central barrel energy(EM-scale) for reconstructed experimental data (circles), reconstructed MC data (triangles) and corresponding MC truth (squares) provided from Calibration Hits. Plots for different beam energies at $\eta = 0.25$ are shown. All data are scaled to 1000 events

23
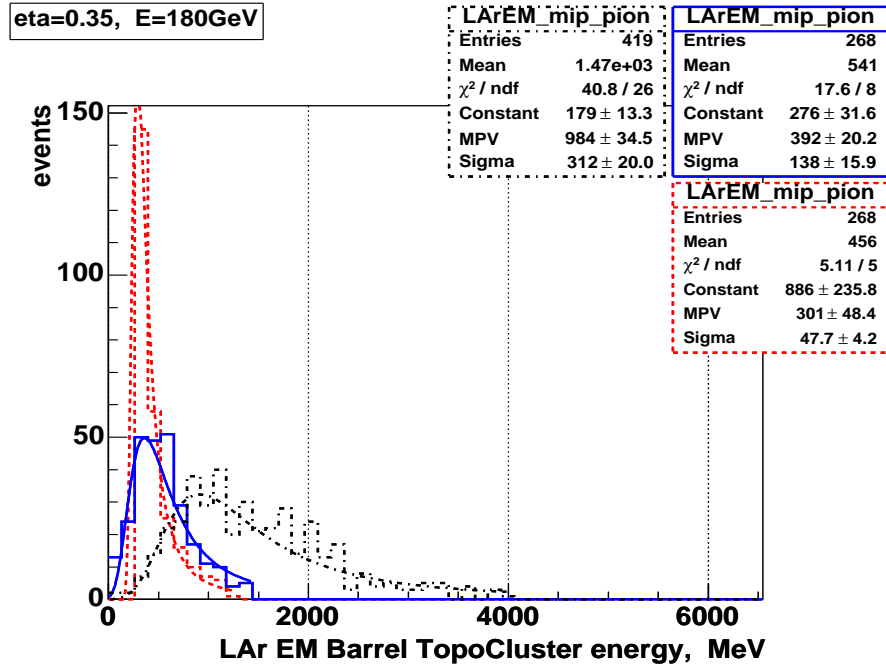
Figure 17: Sum of TopoCluster energies in LAr EM-barrel for MIP like events. Solid line corresponds to MC reconstruction and dash-dotted line to experimental data reconstruction. Dashed line represents MC truth. Results of Landau-fit are also shown. Plots are done for $E_{beam} = 180$ GeV at $\eta = 0.35$.

in LAr EM-barrel for MIP like events. As one can note there is quite big smearing of this energy after reconstruction, especially in case of experimental data.

Fig. 18 shows dependence of MPV (Maximal Probable Value) of MC truth Landau-fit for LAr MIP like events as a function of beam energy at different η. This dependence can be described quite well with linear function slightly increasing with a beam energy,

$$MPV = MPV_0(\eta) + \alpha \cdot E_{beam} \ ,$$

where, $\alpha = 0.0(7) \cdot 10^{-3}$ — appears to be independent on η while MPV_0 increases with η because a pions path in LAr EM barrel increases when η increases.

To select LAr MIP pions we used the following schema. First of all we were taking only the events with total energy in LAr less than some threshold value. Ranges of threshold values were different for different
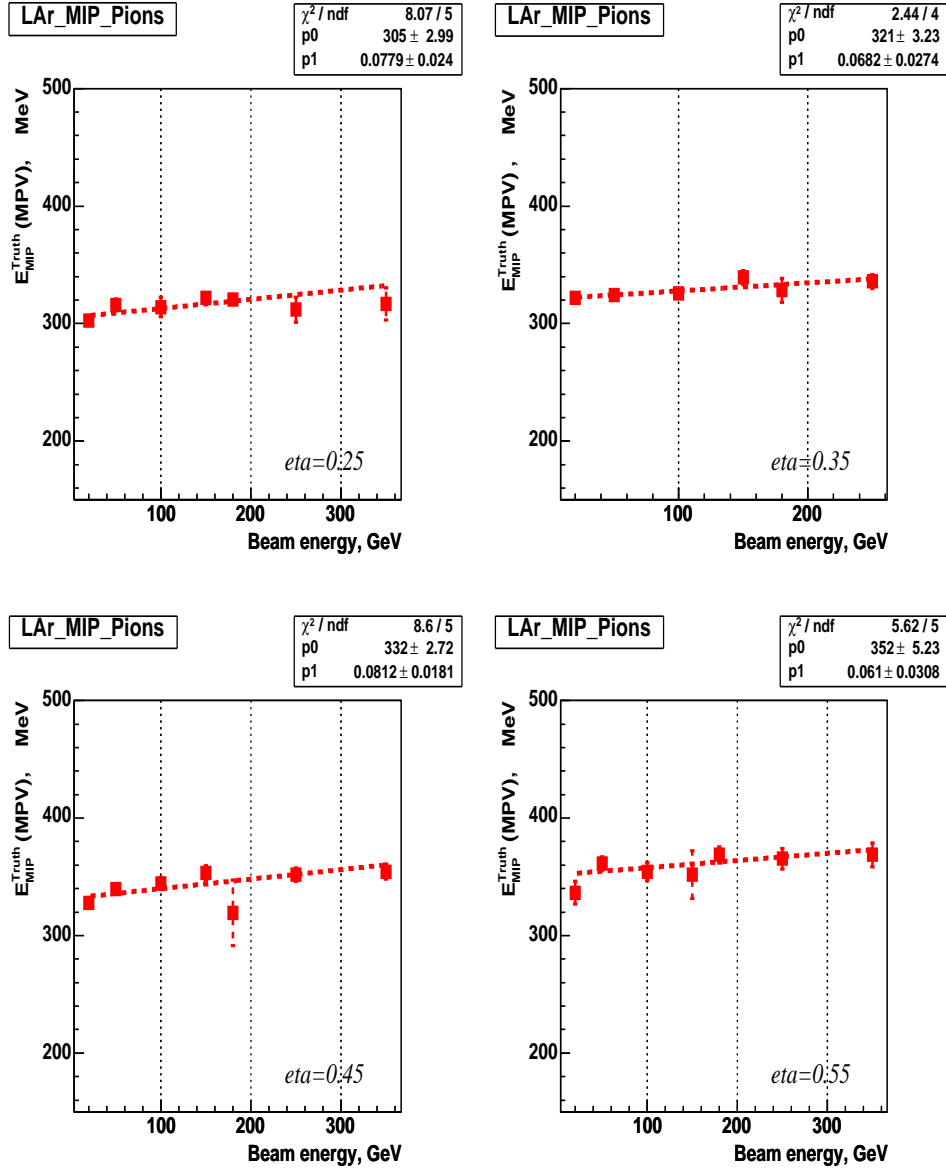
Figure 18: MPV of MC truth Landau-fit as a function of pion beam energy at different η. MC truth for pion energy in LAr EM-barrel is calculated from Calibration Hits for LAr MIP like events.

kind of data (MC truth and experimental reconstructed data). These values are given in Table 4. After that we were applying a criteria on the energy in the last sampling of LAr EM-barrel to be less than in the middle sampling.

Table 4: Upper thresholds of pion energy in LAr EM-barrel for LAr MIP like pions selection. Thresholds are given in GeV units.

η / E_{beam} (GeV)	20	50	100	150	180	250	350
MC truth							
0.25	1.0	1.0	1.0	1.0	1.0	1.5	2.0
0.35	1.0	1.0	1.0	1.0	1.25	1.5	
0.45	1.0	1.0	1.0	1.25	1.25	1.5	2.0
0.55	1.0	1.0	1.25	1.25	1.25	1.5	2.0
Reconstructed CTB2004 data							
0.25	2.0	4.0	4.0	4.0	4.0	4.0	6.0
0.35	3.25		5.0	4.5	4.5	4.5	
0.45	2.5	3.0	3.25	4.0	4.0		
0.55	3.0	4.0	4.0	4.0	4.5		

Fig. 19 provides plots of LAr MIP like pions energy (in EM-scale) distribution in TileCal barrel. Similar to the results without MIP like pion selection shown on the fig. 16, we reached best agreement between MC and experiment at $\eta = 0.25$ for different beam energies in the range of 50 – 350 GeV.

The next fig. 20 shows the results for the TileCal central barrel energy in EM-scale normalized on E_{beam} for the range $E_{beam} = 20 – 350$ GeV and $\eta = 0.25, 0.35, 0.45, 0.55$.

In general, there is a quite good agreement between reconstructed MC and experimental data and between MC reconstruction and MC truth. The difference between reconstructed MC and MC truth varies by less than 2 %. The variation of the difference between MC and experiment is less than 3% if not consider extremely huge differences at $\eta = 0.25$, $E_{beam} = 20$ GeV — $\approx 9\%$ and at $\eta = 0.55$, $E_{beam} = 50$ GeV — $\approx$ 7.5%. These particular cases can be caused by some hardware problems during the corresponding runs or they are the result of some bugs in the reconstruction. Though seeking for true reasons was not among the tasks of this work.

We compared our experimental results for the energy of LAr MIP like pions in TileCal with the results [8] calculated using more precise determination of MIP pions. Our results are systematically less by about
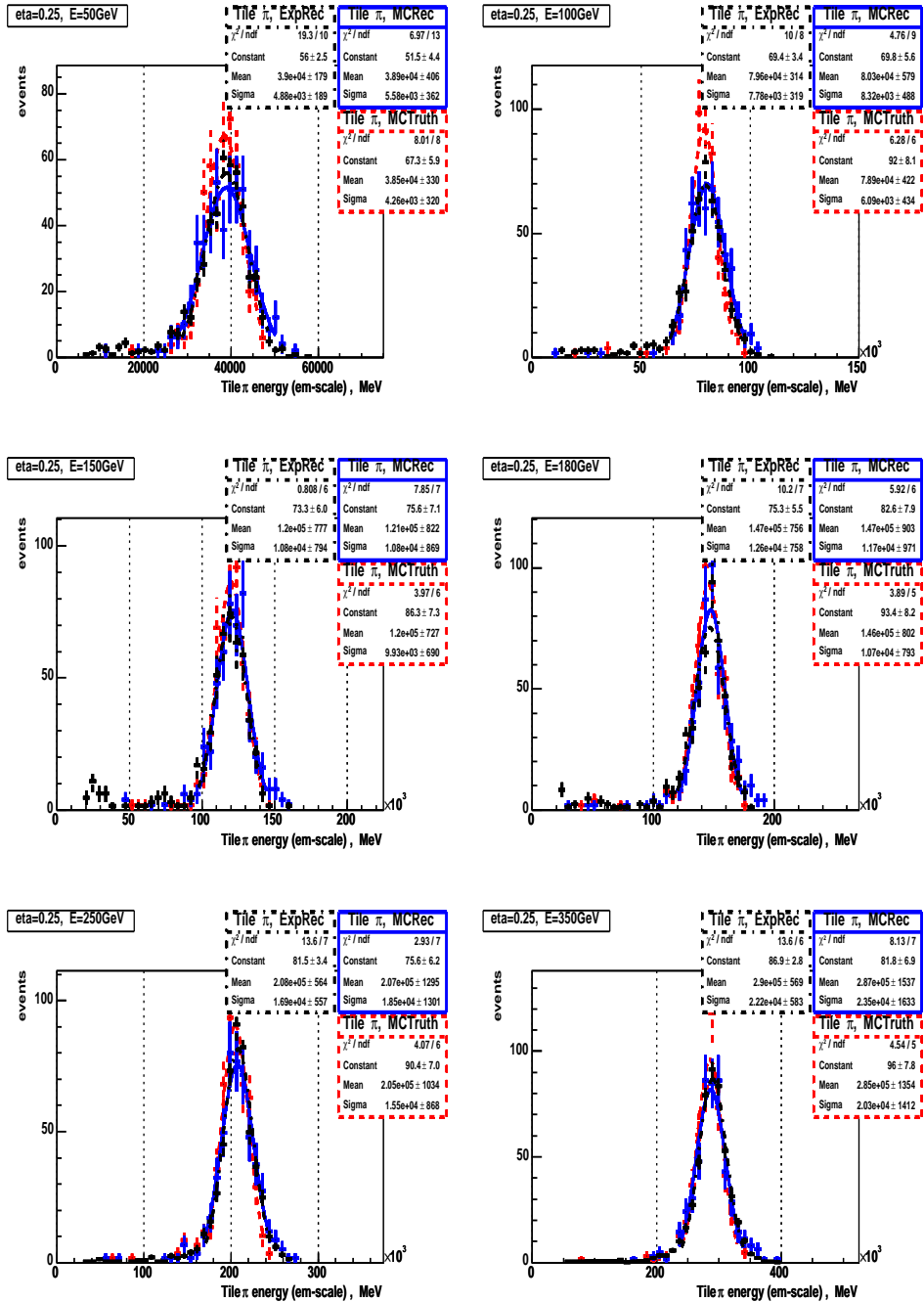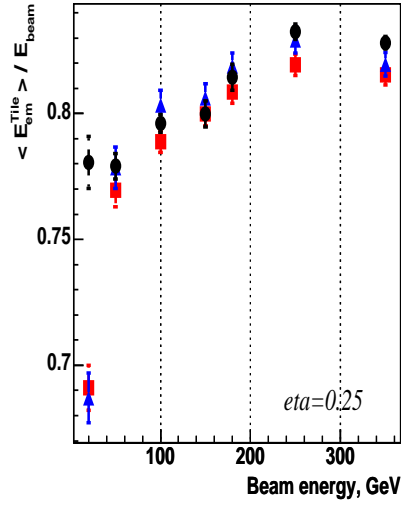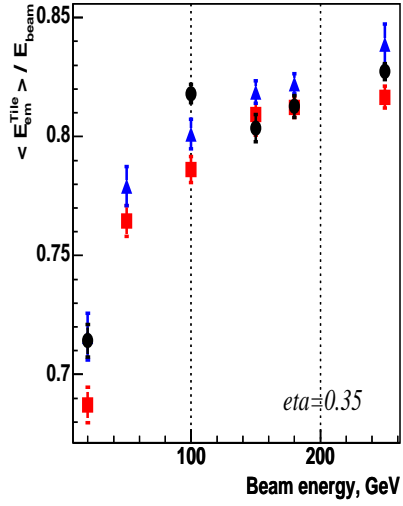
Figure 19: LAr MIP pions energy(em-scale) distribution in TileCal central barrel. Dash-dotted line corresponds to reconstructed experimental data; Solid line corresponds to reconstructed MC data and dashed line is for MC truth. Gauss-fits of these distributions are also shown. Plots are made for different beam energies at $\eta = 0.25$.
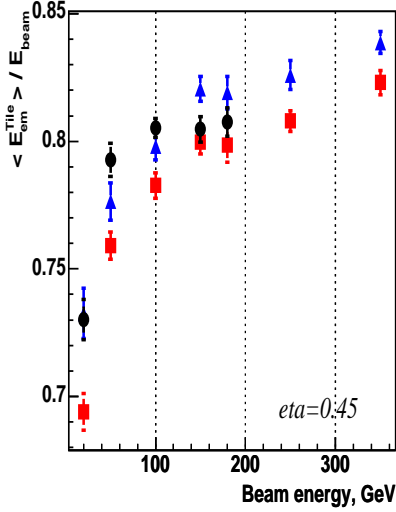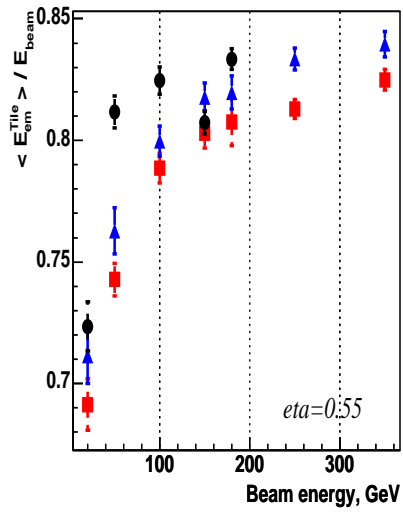
27

Figure 20: Overall picture for LAr MIP like pions energy in TileCal central barrel normalized on E_{beam} for different beam energies and η. Squares represent MC truth, triangles — MC reconstructed response and circles are corresponding to reconstructed experimental response.

$2 - 3$ % what can be explained by the following reasons: a) we were determining MIP in LAr, they — in LAr+Cryostat; b) for reconstruction we were using TopoCluster algorithm, they — their own reconstruction algorithm. Moreover, we did not make the special corrections on protons for the positive pion beams(expected corrections are up to +2% at high energies [9]).

In the time of a preparation of this note there was reported [10] the new results of a comparison of MC to experimental data for whole ATLAS calorimeter, which also showed a good agreement between them for TileCal.

6   Conclusions

In the current work we did calculation of one of the important parameters, Tile Sampling Fraction, used in TileCal Monte-Carlo data reconstruction in TileHit to TileDigit step.

Our calculation of TSF with electrons and pions simulation gave almost the same value for TSF in TileCal central barrel $TSF_{em} = 36.0 \pm 0.3$ and $TSF_{had} = 35.9 \pm 0.4$.

This indicates that non-electromagnetic and electromagnetic parts of hadronic shower contribute in the formation of TileCal response with the same energy sharing between sensitive and absorber materials.

Quite important aspect of this study was the fact that it was first time when special Calibration Hits objects were used, which provide Monte-Carlo truth for an energy distribution in Calorimeter.

Our study of electron response in TileCal showed that an electron response fluctuation strongly depends on pseudo-rapidity. This is the consequence of the same sizes of electrons shower in TileCal modules and the intrinsic non-homogeneous structure of the modules, which is changing with η. We suggest that for TileCal cells calibration in electromagnetic scale (calculation of electromagnetic constants of the cells) it is desirable to take electron scans of the cells only at certain defined η values, which we call "good". At these "good" η-values fluctuation of an electron response is completely Gaussian.

New value, $TSF = 35.9$ significantly improved the agreement between MC truth and MC data reconstruction results for TileCal barrel region. In particular, the event-by-event comparison of these results with accompanying MC truth shows excellent agreement between them.

Comparison of MC results with CTB2004 experimental data was also made. Mostly good agreement between them has been reached, what is the merit of both — the correct MC model and corresponding software and also the good experimental performance in CTB TileCal data

acquisition.

7 Acknowledgments

References

[1] P. Loch, Suggestions for a General Energy Reconstruction Scheme for the ATLAS Calorimeters, ATL-CAL-97-091; ATL-AC-PN-91., 03 Apr 1997, CERN.

[2] Y. Kulchitskii, P. Tsiareshka, V. Vinogradov, Energy Calibration of the TILECAL Modules with the Fit Filter Method (July 2002 Test Beam Data); ATL-TILECAL-PUB-2005-005; CERN.
J. Budagov, J. Khubua, Y. Kulchitskii, N. Rusakovitch, P. Tsiareshka, V. Vinogradov, Electromagnetic Energy Calibration of the TILECAL Modules with the Flat Filter Method (July 2002 Test Beam Data); ATL-TILECAL-PUB-2005-003, CERN.

[3] G. Khoriauli, Talk given on the ATLAS Hadronic Calibration Meeting, 4 March 2004, CERN.
G. Khoriauli, Y. Kulchitsky et al., Talk given on the ATLAS Hadronic Calibration Meeting, 13 May 2004, CERN.
G. Khoriauli, Y. Kulchitsky et al., Talk given on the ATLAS TileCal Software, 29 September 2004, CERN.
A. Solodkov, G. Khoriauli et al., Talk given on the ATLAS Calorimetry Calibration Workshop, 3 December 2004, Tatra, Slovakya.

[4] ATLAS Collaboration, ATLAS Tile Calorimeter Technical Design Report, CERN/LHCC/96-42, 1996, CERN.

[5] C. Padilla, J.Proudfoot, Numerical Calculation of the Sampling Variation intrinsic to the TileCal Scintillator Geometry, TILECAL-NO-073, 10 April 1996.

[6] Particle Data Group, Physics Letters B, 592 (2004) 1-1109.

[7] J.A. Budagov, Y. Kulchitsky et al., ATL-TILECAL 97-127, CERN.

[8] V. Giangiobbe, CTB LAr+Tile pion analysis meeting, CERN, 29 May 2006.

[9] Y. Kulchitskii, S. Tokar, V. Vinogradov, Study of the ATLAS Hadronic Tile Calorimeter non-compensation sensitivity, ATL-COM-TILECAL-2006-004., CERN.

[10] P. Speckmayer, T. Carli, ATLAS Hadronic Calibration Workshop, Munich, 04 May 2006.